

Structure and thermoelectric properties of Cs-Bi-Te alloys fabricated by different routes of reduction of oxide reagents

N. Gostkowska, T. Miruszewski, B. Trawiński, B. Bochentyn, B. Kusz

Gdańsk University of Technology, Faculty of Applied Physics and Mathematics, Solid State Physics Department, ul. G. Narutowicza 11/12, 80-233 Gdańsk, Poland

abstract

Cesium-bismuth-telluride polycrystalline materials were fabricated using a cost-effective method based on a reduction of oxide reagents, leading to a production of a material with good thermoelectric properties. Several samples with various initial stoichiometry were prepared by melting of oxide powders at 1050 °C, quenching, milling to powders and then reducing in pure hydrogen at 400 °C. Another concept was to obtain the CsBi₄Te₆ material without a melting stage. Composition of the samples was analyzed by the XRD and EDX methods. The sample with 96% of CsBi₄Te₆ phase was obtained in a way of reduction of oxide reagents. Thermoelectric properties of fabricated samples were also investigated.

Keywords: Oxide materials, Thermoelectric, Solid state reaction, Alloy

1. Introduction

Thermoelectric (TE) materials are very promising candidates for renewable energy resources as they are able to convert heat directly into electricity. However, low efficiency of devices based on TE materials hinders their applications even in a wide range of temperatures. Thermoelectric efficiency of a material is described by thermoelectric figure of merit (ZT), defined as:

$$ZT = \frac{\alpha^2 \sigma}{\kappa_{tot}} T \quad (1)$$

where α - Seebeck coefficient, σ - electrical conductivity, κ_{tot} - total thermal conductivity, T - absolute temperature in Kelvin. As can be seen, the figure of merit (ZT) increases with both Seebeck coefficient and electrical conductivity, but also decreases proportionally to the thermal conductivity κ_{tot} . The numerator ($\alpha^2 \sigma$) is called power factor (p_f) and should reach high values. However α as well as σ are inversely related (see Eq. (1)) so a compromise between these two values should be achieved in order to obtain a promising TE material. Another important parameter is a thermal conductivity which should be as low as possible. The total thermal conductivity

is a sum of an electronic component κ_e and a lattice component κ_L ($\kappa_{tot} = \kappa_e + \kappa_L$). The κ_e is strongly connected with carrier transport. Thus, if electrical conductivity of an analyzed material is high, its electrical thermal conductivity also reaches high values. The electrical component κ_e can be described by the Wiedemann-Franz relationship,

$$\kappa_e = L_0 T \sigma \quad (2)$$

where T is a temperature in Kelvin, σ is an electrical conductivity and L_0 is the Lorentz constant equal to $2.45 \cdot 10^{-8} \text{ W}\Omega\text{K}^{-2}$ which was used for calculations for crystals [1]. Lattice component κ_L is related to the mean free path of phonons which strongly depends on a structure of the material and a concentration of defects. High values of the power factor (p_f) and at the same time low thermal conductivity may be obtained in materials with a complex composition and structure. A perfect thermoelectric material should be a narrow-bandgap semiconductor with highly mobile carriers [2].

TE compounds with different composition and structure can be found in the literature: PbTe [3], bismuth telluride compounds [4,5], TAGS [6], SiGe [7], CoSb₃ [8], Ge clathrates [9], AgSbTe₂ [10], but only few materials exhibit desired thermoelectric properties at low temperatures [11,12].

CsBi₄Te₆ material is one of the best thermoelectric materials among these which operate at low-temperatures. This compound has a *C2/m* space group and a structure composed of Bi₄Te₆ anionic

layers and Cs^{1+} ions residing between the layers. It also contains rare Bi^{2+} ions that form novel Bi-Bi bonds. The CsBi_4Te_6 crystals have needle-like morphology. The strong charge transport anisotropy [13] and different sign of the Seebeck coefficient along c-axis and b-axis direction was observed in this material [1]. B-axis of the crystal is a preferable direction characterizing with the best thermoelectric performance [1]. An „as-prepared” compound is a p-type semiconductor. The room temperature conductivity of its crystals changes in a range of 450–900 S/cm and thermopower values are in the range of 90–150 $\mu\text{V/K}$. The CsBi_4Te_6 crystals have a thermal conductivity of around 1.8 W/mK at room temperature [1], and κ values of polycrystalline samples are similar [14]. The doping process has a strong influence on the thermoelectric properties which leads to both p-type and n-type material. Depending on the type and percent of used dopants, a different sign of the Seebeck coefficient may be observed. The highest $ZT = 0.82$ was achieved at -48°C for p-type crystals by SbI_3 doping [1].

Different fabrication methods have been reported for obtaining thermoelectric materials. Mechanical milling process using pure metals as raw materials is the most commonly used [15]. The process usually contains hot pressing [16] or spark plasma sintering stage [17,18] to form a polycrystalline material. A PVD [19] and CVD [20] process is also used to produce thin films of thermoelectric materials. For fabrication of a single phase CsBi_4Te_6 material some other experimental methods can be found in the literature. D. Chung and T. Hogan [1] have obtained CsBi_4Te_6 single crystals by reacting Cs_2Te with Bi_2Te_3 or Cs with Bi_2Te_3 at different temperatures, from 250°C to 700°C . These methods require special fabrication techniques and a usage of an expensive and reactive Cs substrate.

A. Datta and G. S. Nolas [14] reported a Seebeck coefficient equal to $-47 \mu\text{V/K}$ and an electrical conductivity equal to 22 S/cm at room temperature and they have not observed a p-n transformation at -261°C – -27°C temperature range. This research group used a low temperature solvothermal process for the synthesis of CsBi_4Te_6 crystals. They used cesium acetate, bismuth nitrate and sodium tellurite as precursors. TetraEG was used as the solvent and NaBH_4 as the reducing agent. The mixture was then ultrasonicated for 30 min and NaBH_4 has been added. The solution was put in an oven at 200°C for 16 h to complete the reaction. Obtained product was then ground to powder, and the densification was achieved by Spark Plasma Sintering.

H. Lin et al. [21] synthesized a polycrystalline compound. The synthesis process was done with a usage of a praseodymium rare earth element as the reducing reagent for the solid-state reaction with Bi, Te and CsCl flux at 900°C . Rare earth metals are quite expensive and may introduce additional impurity to the structure. Surprisingly, they observed a change in the sign of the Seebeck coefficient for their polycrystalline samples (from positive to negative), reaching $-76 \mu\text{V/K}$ at around 370°C while the measured electrical conductivity of the sample is 377 S/cm. A maximum value of ZT equal to 0.14 was noticed at 362°C , which is a relatively high temperature for CsBi_4Te_6 compound.

The aim of this paper was to obtain a polycrystalline CsBi_4Te_6 material in a simple and cheap way that would enable the large scale production. Although a single crystalline material could exhibit better properties, a polycrystalline material will be cheaper and easier to produce in terms of a mass production. A method for thermoelectric material fabrication using oxide powders was proposed and used to synthesize the CsBi_4Te_6 materials. The temperatures used in this method are relatively low, comparing to the SPS or hot pressing fabrication technique. It also requires the usage of oxide powders as reagents, in contrast to the mechanical milling method which requires pure metals as reagents. The process of reduction of oxide reagents was previously described in the

literature [22–25]. It is known, that the initial nonstoichiometry can increase the amount of precipitations. The temperature and the duration time of the reduction process may have a great influence on the final composition, porosity and the structure of analyzed samples. In this paper, we present a thermoelectric characterization of the low-temperature CsBi_4Te_6 compound, fabricated from oxide reagents (with or without the melting stage) which were reduced in hydrogen.

2. Experimental details

The first concept was to obtain a CsBi_4Te_6 thermoelectric material by a reduction of melted oxides (called as MO in this paper). Samples with a composition $\text{Cs}_x\text{Bi}_4\text{Te}_6\text{O}_y$ (where $x = 1$ and 1.1) have been produced from an appropriate amount of oxides (Bi_2O_3 , TeO_2 , both Alfa Aesar, 99.99%) and cesium carbonate (Sigma Aldrich, 99.99%). The powders were then mixed in order to obtain a stoichiometric sample ($\text{CsBi}_4\text{Te}_6 - \text{MO}$) and a sample with an excess of cesium ($\text{Cs}_{1.1}\text{Bi}_4\text{Te}_6 - \text{MO}$). In a next step the powders were melted at 1050°C and quenched in air. 1050°C is a temperature at which the oxides were in a liquid state. A decomposition of cesium carbonate was observed. The obtained polycrystalline material was ground and uniaxially pressed under a pressure equal to 350 MPa. Bulk cylindrical pellets were obtained and reduced in hydrogen at 400°C for 10 h. After preliminary reduction, pellets were subsequently ground and pressed under a pressure equal to 700 MPa. Finally, the samples were reduced at 400°C for 10 h in hydrogen once again.

Another route to produce the TE material was a conventional solid state reaction (called as SSR in this paper) in hydrogen. The appropriate oxides and cesium carbonate were mixed to obtain a composition: $\text{Cs}_x\text{Bi}_4\text{Te}_6\text{O}_y$ (where $x = 1$ and 1.1). The two different samples were obtained: stoichiometric ($\text{CsBi}_4\text{Te}_6\text{-SSR}$) and with an excess of cesium ($\text{Cs}_{1.1}\text{Bi}_4\text{Te}_6 - \text{SSR}$). $\text{CsBi}_4\text{Te}_6\text{-SSR}$ sample was placed in ball milling bowls and ground with ZrO_2 balls in isopropanol for 10 h at 300 rpm. The powders were then pressed under a pressure equal to 350 MPa and reduced in hydrogen at 400°C for 10 h. After this process, the samples were ground, pressed under pressure equal to 700 MPa and sintered in hydrogen under the same conditions. The process was repeated once more and then samples ready to study TE properties were obtained.

The phase composition of the investigated materials was analyzed using the X-ray diffraction method by an X'Pert Pro MPD Philips diffractometer with $\text{Cu K}\alpha$ (1.542 Å) radiation at room temperature. The XRD patterns were also analyzed by the Rietveld refinement method using a PANalytical HighScore Plus 3.0b program with the pseudo-Voigt profile function applied.

The morphology of samples was analyzed by FEI Quanta FEG 250 Scanning Electron Microscope (SEM) with a secondary electron detector operating in a high vacuum mode with the accelerating voltage 20 kV. For SEM observations samples were covered with a 15 nm - thick layer of gold. A quantitative analysis using the Energy Dispersive X-ray Spectroscopy by EDAX Genesis APEX 2i with ApolloX SDD spectrometer was also performed. The samples for the EDX analysis were prepared by an immersion in the resin, grinding and polishing.

The electrical conductivity (σ) of bulk cylindrical samples was measured using a 4-wire method in a temperature range from -100 to 100°C in argon atmosphere. The 10% measurement uncertainty was assumed. To investigate the impact of porosity on the measured electrical conductivity we calculated the porosity corrected σ_{cor} values using the Bruggeman expression [26].

$$\sigma_{\text{cor}} = \sigma(1-p)^{-3/2} \quad (3)$$

where σ is the measured electrical conductivity and p is the porosity of the samples.

The Seebeck coefficient was measured on the basis of voltage measurements in contacts between the sample and two copper blocks presenting a known temperature difference. The Seebeck coefficient was measured with a 5% uncertainty and presented in reference to Pt.

The total thermal conductivity was determined in a temperature range of 32–38 °C using a homemade equipment operating in vacuum conditions. Measurement is based on the analysis of heat transfer between two copper blocks. In this case, the 10% measurement uncertainty was assumed. The Klemens formula [27] was used in order to correct the influence of porosity on total thermal conductivity, according to the equation:

$$\frac{\kappa_{tot}}{\kappa} = 1 - \frac{4}{3}p \quad (5)$$

where κ_{tot} is corrected value, κ measured and p is porosity. Corrected values of total thermal and electrical conductivity were used to estimate the electronic part of thermal conductivity with Wiedemann-Franz formula. The lattice part of thermal conductivity (κ_L) was determined as the difference between the total thermal conductivity (κ_{tot}) and electronic part of thermal conductivity κ_e . Density of samples was determined using Archimedes' method.

3. Results and discussion

In order to compare the structure of CsBi_4Te_6 materials depending on the synthesis method and Cs stoichiometry, the XRD measurements were performed. Fig. 1a presents the XRD patterns of CsBi_4Te_6 and $\text{Cs}_{1.1}\text{Bi}_4\text{Te}_6$ samples fabricated by a solid state synthesis method. The XRD patterns of CsBi_4Te_6 samples fabricated by reduction of melting oxides (MO) with and without cesium excess in the structure are presented in Fig. 1b. The results in Fig. 1a show that almost all indexed peaks can be attributed to the monoclinic $C2/m$ CsBi_4Te_6 phase. However, an additional peaks representing Bi_2Te_3 phase can be found. A comparison between CsBi_4Te_6 and $\text{Cs}_{1.1}\text{Bi}_4\text{Te}_6$ structures fabricated by SSR method is also presented in this figure. The obtained results indicate that additional amount of Cs in the structure causes an increase of the amount of CsBi_4Te_6 phase. It is also visible as an increase of intensity of a characteristic peak at 28.3° (indicated by an arrow) which is responsible for the existence of the CsBi_4Te_6 phase.

Fig. 1b shows a comparison of XRD patterns of CsBi_4Te_6 and $\text{Cs}_{1.1}\text{Bi}_4\text{Te}_6$ samples fabricated in a way of reduction of melted oxides (MO) at 1050 °C. As can be seen in case of CsBi_4Te_6 -MO (melted oxides) sample, almost all indexed peaks can be attributed to the monoclinic $C2/m$ CsBi_4Te_6 phase. However, some additional peaks representing Bi_2Te_3 phase can also be found. The Rietveld analysis of this pattern showed, that the weight fraction of visible phases CsBi_4Te_6 : Bi_2Te_3 is 83%: 17% what indicates, that the predominant phase in this sample is CsBi_4Te_6 . However authors believe that the presence of Bi_2Te_3 phase in this sample may have a strong influence on the thermoelectrical properties. Generally speaking, it is possible to obtain a thermoelectric CsBi_4Te_6 material by a reduction of oxides.

The structural data obtained from Rietveld analysis is presented in Table 1. These results showed also that the additional amount of Cs caused an increase of CsBi_4Te_6 phase from 83% to 93%. In consequence, the characteristic peak visible at 28.3° which is responsible for the existence of pure CsBi_4Te_6 phase increased. As can be also seen, the significant amount of rhombohedral $R\bar{3}m$ bismuth telluride phase was observed in CsBi_4Te_6 - MO sample. In case of $\text{Cs}_{1.1}\text{Bi}_4\text{Te}_6$ - MO material the amount of bismuth telluride

was estimated to be around 7%, thus, it decreased in comparison to the sample without the Cs excess in the structure.

The comparison of XRD patterns of the samples with Cs excess in the structure which were sintered by different routes - $\text{Cs}_{1.1}\text{Bi}_4\text{Te}_6$ -SSR (Fig. 1a) and $\text{Cs}_{1.1}\text{Bi}_4\text{Te}_6$ -MO (Fig. 1b) enable to draw further conclusions. It can be seen that the phase composition of these samples is quite similar (see Table 1). In both samples the monoclinic $C2/m$ CsBi_4Te_6 is visible as a predominant phase and some additional peaks representing bismuth telluride phase can be found. However, an increase of the characteristic CsBi_4Te_6 peak visible at 28.3° in case of $\text{Cs}_{1.1}\text{Bi}_4\text{Te}_6$ -SSR sample is also interesting. This may indicate that the CsBi_4Te_6 monoclinic phase amount in this sample may be higher than in $\text{Cs}_{1.1}\text{Bi}_4\text{Te}_6$ -MO. It was also proved by the Rietveld analysis. Therefore, authors suggest that the solid state reaction method may be more favorable for obtaining CsBi_4Te_6 thermoelectric materials. Moreover, in case of a reduction of melted oxides method authors expect an additional non-stoichiometry in samples due to the probable partial evaporation of Bi and Te, caused by a high fabrication temperature equal to 1050 °C.

In order to analyze the composition of obtained TE materials, the EDX measurements were performed. The results showed that there is a nonstoichiometry in analyzed samples. In samples prepared by a reduction of melted oxides a significant deficiency of cesium was observed. The stoichiometry of the CsBi_4Te_6 -SSR sample calculated from the EDX analysis was $\text{Cs}_{1.2}\text{Bi}_{3.2}\text{Te}_6$, and a deficiency of bismuth was observed in all samples. For comparison the EDX measurement of a Bi_2Te_3 reference sample which was reduced in the same conditions as CsBi_4Te_6 was performed. It revealed a $\text{Bi}_{1.6}\text{Te}_3$ stoichiometry of initial Bi_2Te_3 sample which is a result of the evaporation of bismuth during the reduction process [22]. Because of the depletion with bismuth in fabricated samples, the stoichiometry calculated from EDX analysis was normalized to tellurium.

In literature reports a quantitative analysis was performed on CsBi_4Te_6 crystals by D. Chung and T. Hogan [1]. They reported an average stoichiometry equal to $\text{Cs}_{0.96}\text{Bi}_4\text{Te}_{6.6}$. If this stoichiometry was normalized to tellurium as we do it in this paper, it will give a stoichiometry equal to $\text{Cs}_{0.87}\text{Bi}_{3.64}\text{Te}_6$ which shows significant deficiency of bismuth in crystals, probably due to the high temperature during synthesis process resulting in an evaporation of bismuth. This result is in agreement with our observations.

The morphology of obtained samples was investigated by a Scanning Electron Microscopy (SEM). Fig. 2 presents SEM images of the analyzed samples. The micrographs show polycrystalline material with several pores of micrometer size. Fig. 2a shows the microstructure of CsBi_4Te_6 -SSR sample. Structures of different size can be found in the sample. The grain shape is different and pore distribution is also irregular.

Fig. 2b presents the SEM image of a CsBi_4Te_6 -MO sample, for which a very low thermal conductivity was noticed (0.43 W/mK). The SEM image shows a multiphase spot where the grains with very various shape and size occur. The grain composition may differ, hence the different shape of the grains can be found in the picture. A non-uniform structure may be caused by a high temperature fabrication method. During melting of oxides a partial crystallization of a melt may occur, which will result in a less uniform structure than in the case of a sample fabricated by SSR method. Moreover, the XRD analysis revealed that Bi_2Te_3 phase is present, thus it can be stated that the sample is a composite of CsBi_4Te_6 and Bi_2Te_3 . The Cs-Te based phases may also occur and affect the final thermoelectric properties of the composite.

The $\text{Cs}_{1.1}\text{Bi}_4\text{Te}_6$ samples obtained by SSR and MO methods are presented in Fig. 2c and d, respectively. These samples have the highest content of CsBi_4Te_6 phase calculated from the XRD

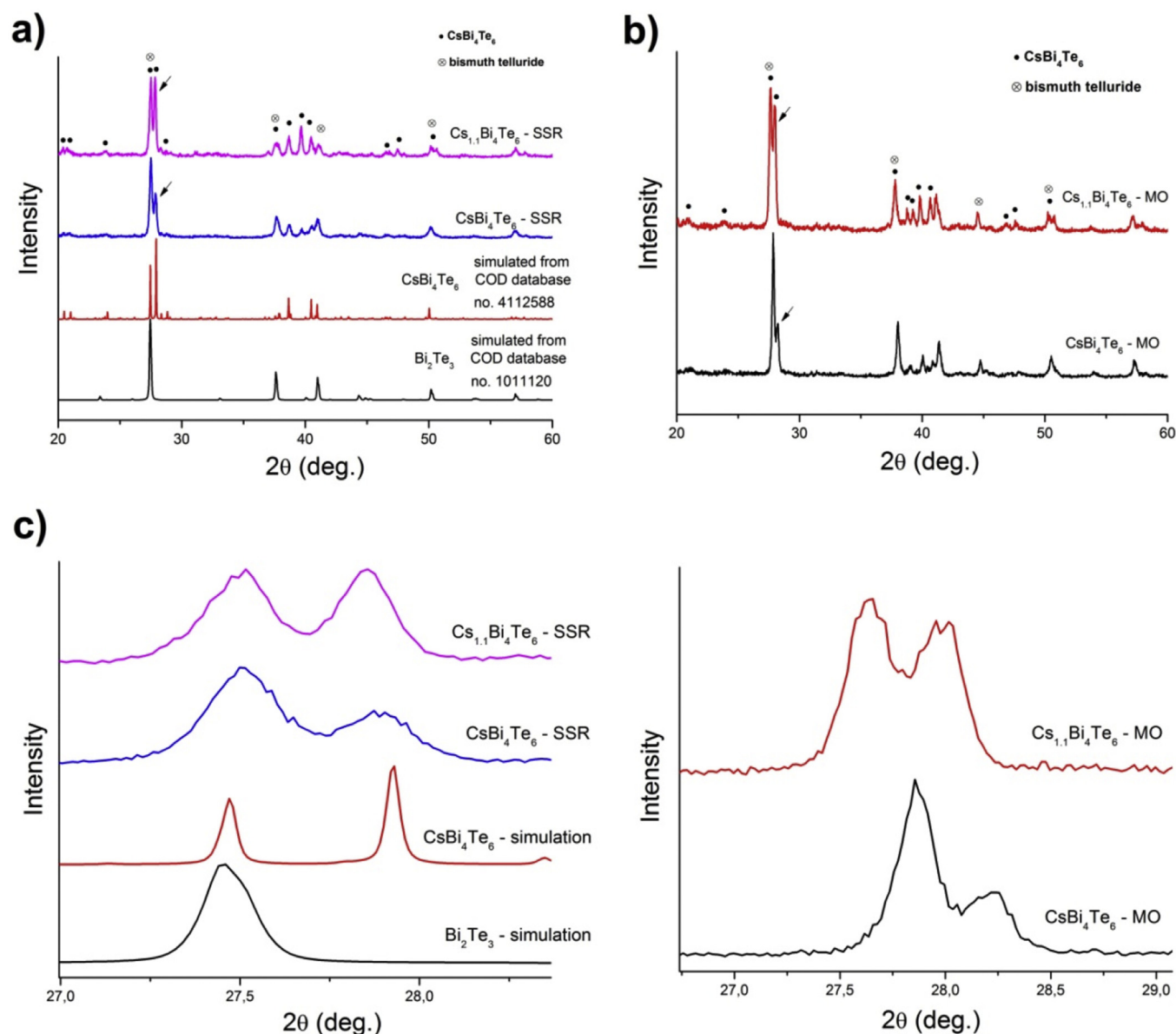


Fig. 1. XRD patterns presenting a) CsBi_4Te_6 and $\text{Cs}_{1.1}\text{Bi}_4\text{Te}_6$ samples sintered by SSR method in hydrogen; b) CsBi_4Te_6 and $\text{Cs}_{1.1}\text{Bi}_4\text{Te}_6$ samples sintered by reduction of melted oxides method. The characteristic 28.3° CsBi_4Te_6 peaks are indicated by arrows in these figures. The characteristic peaks are also enlarged in Fig. 1c. The simulated CsBi_4Te_6 (COD database 4112588) and Bi_2Te_3 (COD database 1011120) patterns are shown in Fig. 1a as reference structures.

Table 1
Summary of structural properties of CsBi_4Te_6 -MO, $\text{Cs}_{1.1}\text{Bi}_4\text{Te}_6$ -MO and $\text{Cs}_{1.1}\text{Bi}_4\text{Te}_6$ -SSR samples.

| Formula | CsBi_4Te_6 -MO | $\text{Cs}_{1.1}\text{Bi}_4\text{Te}_6$ -MO | $\text{Cs}_{1.1}\text{Bi}_4\text{Te}_6$ -SSR |
|-----------------------------|--------------------------------|---|--|
| Weight content of phase [%] | | | |
| CsBi_4Te_6 | 83% | 93% | 96% |
| Bi_2Te_3 | 17% | 7% | 4% |
| Space group | C2/m | C2/m | C2/m |
| a (Å) | 51.945 (2) | 51.933 (3) | 51.956 (2) |
| b (Å) | 4.4041 (1) | 4.4721 (2) | 4.4266 (2) |
| c (Å) | 14.5311 (2) | 14.5211 (1) | 14.5298 (2) |
| β (deg.) | 100.567 (1) | 101.575 (1) | 101.773 (1) |

measurements. The $\text{Cs}_{1.1}\text{Bi}_4\text{Te}_6$ -SSR sample has a homogeneous structure and longitudinal crystals can be found in it. For comparison, the grains that can be seen in the $\text{Cs}_{1.1}\text{Bi}_4\text{Te}_6$ -MO sample are sharp and placed irregularly what may be a consequence of the

melting stage.

The total electrical conductivity of all samples was measured in a temperature range from -100°C to 100°C (Fig. 3). The results of CsBi_4Te_6 -MO sample indicate a nondegenerate semiconducting behavior, while the results obtained for the others show a degenerate semiconducting behavior. The observed temperature dependence of electrical conductivity in these samples is relatively weak. On the other hand, the different behavior of one sample may be due to its composite-like structure since, according to the XRD, the Bi_2Te_3 : CsBi_4Te_6 phase ratio is significantly higher than in other samples. Basically, the samples sintered by SSR method exhibit higher values of electrical conductivity. The highest values of σ are observed for the CsBi_4Te_6 -SSR sample. They change in a range from 363 to 400 S/cm.

Except of the electrical conductivity, the Seebeck coefficient was also measured in a wide temperature range. The results are shown in Fig. 4. The negative sign of α indicates an n-type conduction

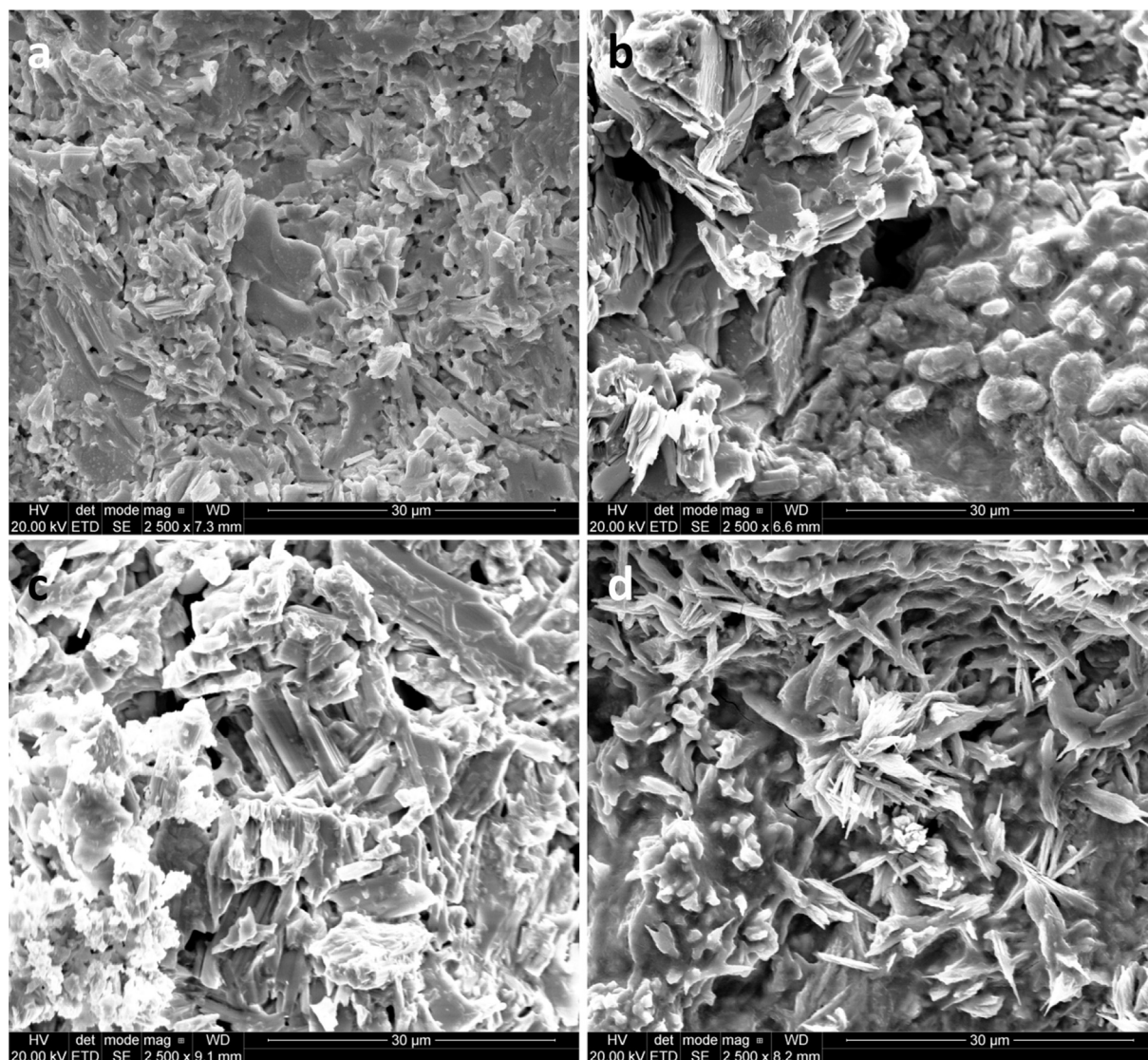


Fig. 2. SEM images of fabricated samples a) CsBi_4Te_6 – SSR, b) CsBi_4Te_6 – MO, c) $\text{Cs}_{1.1}\text{Bi}_4\text{Te}_6$ – SSR, d) $\text{Cs}_{1.1}\text{Bi}_4\text{Te}_6$ – MO.

mechanism in analyzed compositions. It is caused by a slight decrease in concentration of Bi in relation to Te as a result of Bi evaporation during the reduction process. The deficiency of bismuth was observed in all of the analyzed samples. In that case, substitution of Te for Bi leads to creation of an electron carrier [1] and n-type doping. The lowest value of α is observed for a CsBi_4Te_6 –MO sample around 100 °C ($\alpha = -84 \mu\text{V}/\text{K}$). The sample with the highest amount of CsBi_4Te_6 phase ($\text{Cs}_{1.1}\text{Bi}_4\text{Te}_6$ –SSR) has a low value of thermopower factor, while the other samples (CsBi_4Te_6 –SSR and $\text{Cs}_{1.1}\text{Bi}_4\text{Te}_6$ –MO) present comparable values or even higher than reported in the literature for other polycrystalline compounds in an investigated temperature range [14,21]. The thermopower values of CsBi_4Te_6 –MO sample decreases rapidly from -12 to $-84 \mu\text{V}/\text{K}$ in the investigated temperature range. The reason for such behavior is that 17% of the Bi_2Te_3 phase in the structure of the composite may have the positive and strong influence on the thermoelectric properties, especially at higher temperatures. We suppose that in this multi-phase polycrystalline material, the Bi_2Te_3 phase is determining the electrical properties of the sample. The Bi_2Te_3 phase existence manifest in the increase of the ZT with the temperature and the maximum is expected above the 150 °C which

is not characteristic for the low-temperature CsBi_4Te_6 phase. Similar effect may have been occurred by H. Lin et al. [21] in their investigations.

A temperature dependence of a power factor in fabricated samples is presented in Fig. 5. The highest p_F value equal to $138 \mu\text{W}/\text{mK}^2$ is observed for CsBi_4Te_6 –MO sample at 100 °C.

The relative density of samples along with thermal conductivity values and calculated thermoelectric figure of merit (ZT) are presented in Table 2. The results of relative density of the samples, calculated against theoretical value of CsBi_4Te_6 equal to $7.088 \text{ g}/\text{cm}^3$, is consistent with a porosity of samples, which is visible in SEM images (Fig. 2). Thermal conductivity was determined at 32–38 °C. The measured values are lower than these obtained by A. Datta and G. S. Nolas [14]. The values obtained in this work indicate that the lattice thermal conductivity has a major contribution to the κ_{tot} . Finally, the ZT parameter was determined also at 32–38 °C. The results shown for CsBi_4Te_6 – MO sample reveals surprisingly low thermal conductivity equal to $0.43 \text{ W}/\text{mK}$, resulting in the highest ZT value. The complex structure of the CsBi_4Te_6 –MO sample with traces of other phases may be responsible for the very low κ value, however possible internal crack in the sample may affect the final

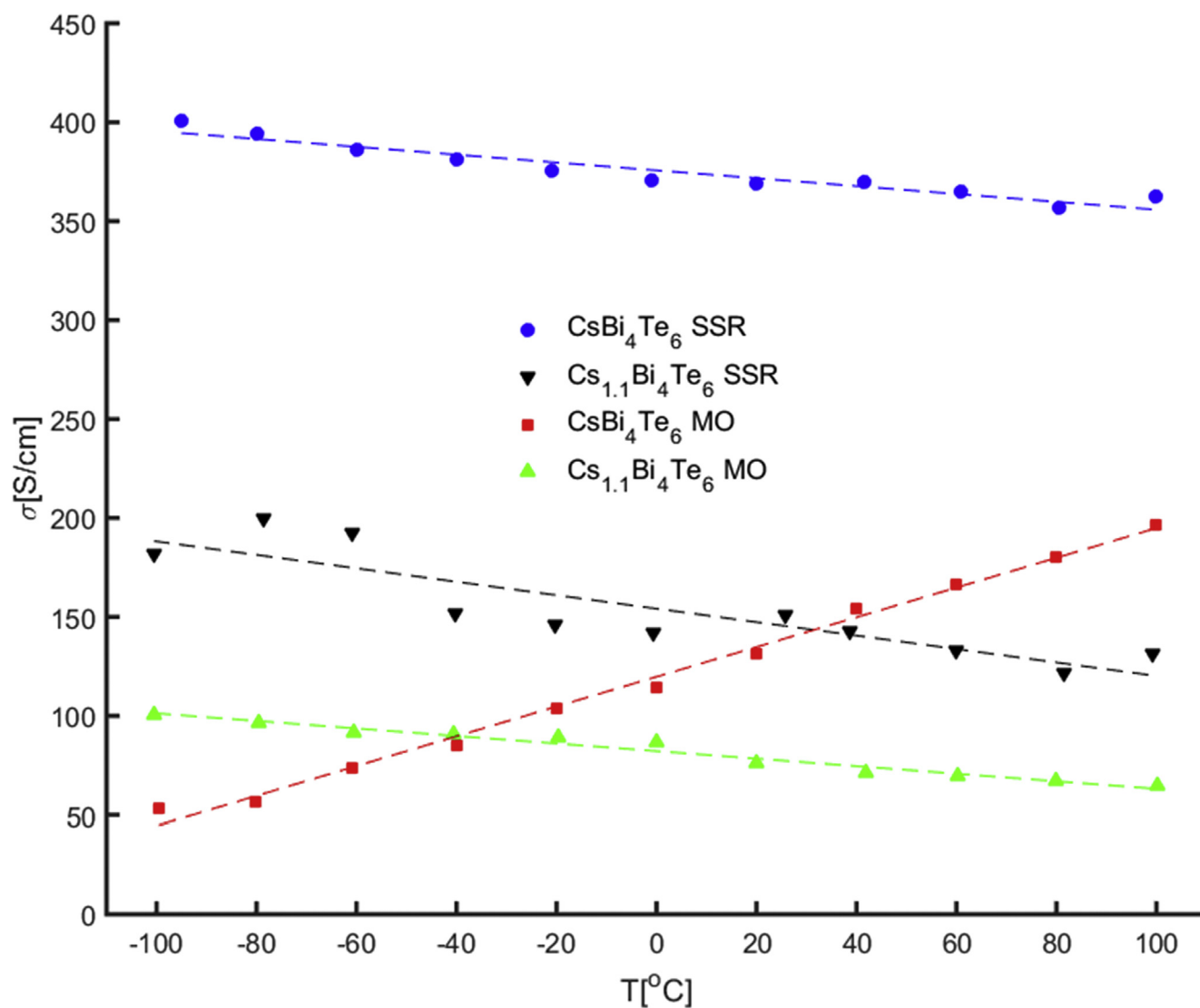


Fig. 3. Temperature dependence of a total electrical conductivity of CsBi₄Te₆ samples. Solid lines are guide for eyes only.

result. It may be also responsible for a nondegenerate semi-conducting behavior of the material.

The investigations of aging effect were also performed. After few days to couple of weeks exposure to H₂O in air, the Cs loss in the structure was observed and cesium hydroxide precipitate was formed on the surface of the sample. Fig. 6 presents a SEM image of the sample where longitudinal structures can be observed. The EDX spectrum of marked spot revealed that Cs is the main component of the structure and neither Bi nor Te was found in it. This probably caused a decomposition of the CsBi₄Te₆ compound. This observation explains also, why the excess of Cs was formed in the results of prior EDX analysis, which is actually a surface method. Thus, the potential application of the material obtained by reduction of oxides should prevent exposure to air.

4. Conclusions

Two methods of CsBi₄Te₆ materials fabrication were presented in this paper. Samples were obtained by reduction of oxide materials in hydrogen atmosphere at 400 °C. The materials were received by two different routes, from oxides which were melted at

1050 °C and mixed and compressed oxides.

The authors obtained the polycrystalline samples with 96% amount of CsBi₄Te₆ phase using a simple, low-cost and low temperature method. The XRD analysis revealed that samples with an excess of cesium in initial composition had the largest amount of CsBi₄Te₆ phase. To improve TE properties of these materials further optimization through doping is required. It is believed that the excess of cesium is needed to obtain a single CsBi₄Te₆ phase. In addition, the melting of oxides stage causes a loss of cesium, which can be compensated by an excess of Cs used in initial composition of the sample. Thus it is stated that with appropriate initial composition of the oxide materials and with the excess of cesium it is possible to obtain a 100% CsBi₄Te₆ phase n-type material using the reduction of oxide reagents method. On the basis of other TE materials investigations [23] we know, that Sb or Sn doping is easy in the reduction of the oxides method and may significantly increase ZT values [1].

It is worth to underline, that the density of the samples is less than the theoretical value which affects the values of the electrical conductivity. Pressing at higher temperatures, for example, by SPS method, should increase the values of the electrical conductivity

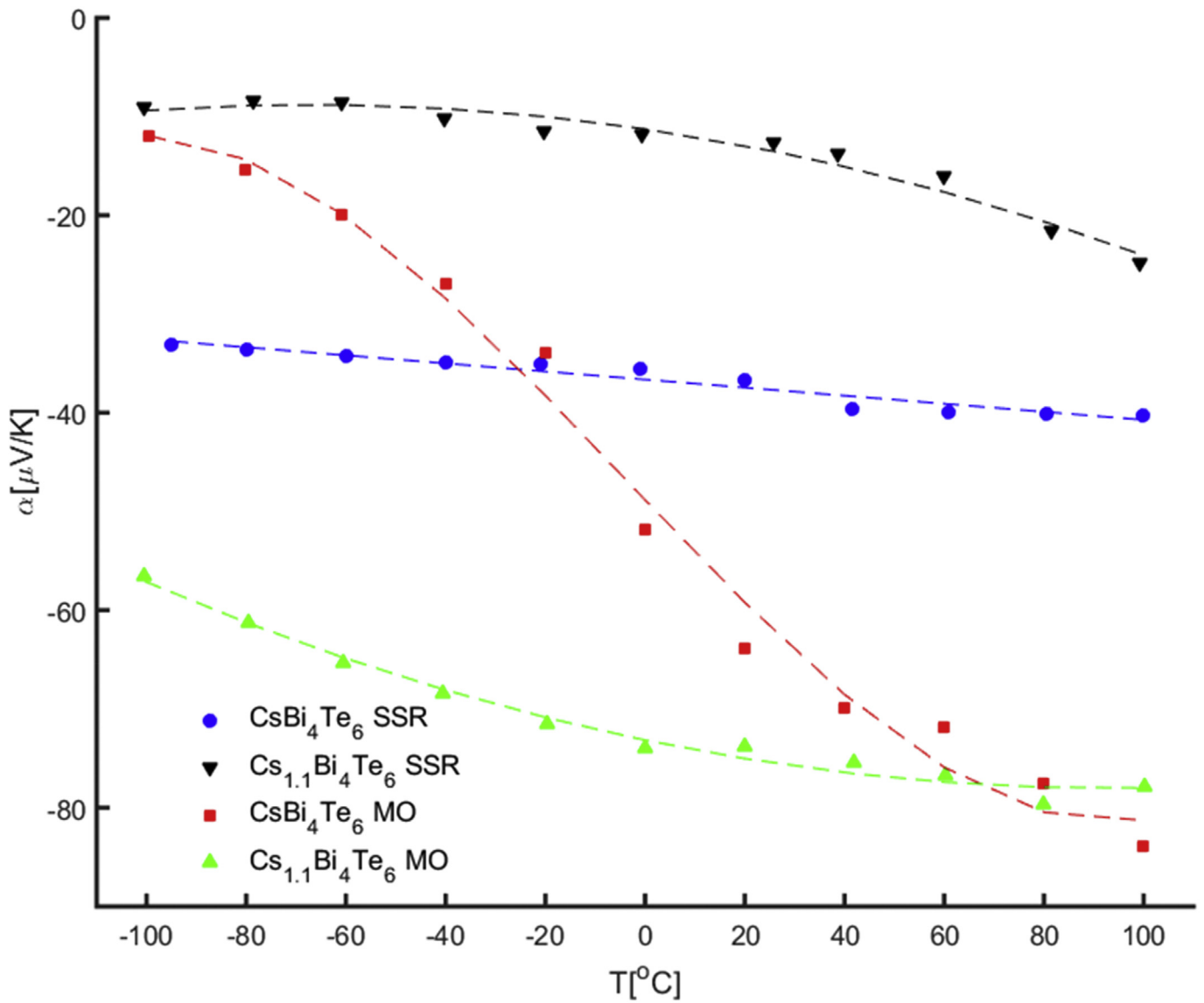


Fig. 4. Temperature dependence of Seebeck coefficient measured for different samples. Solid lines are guides for eyes only.

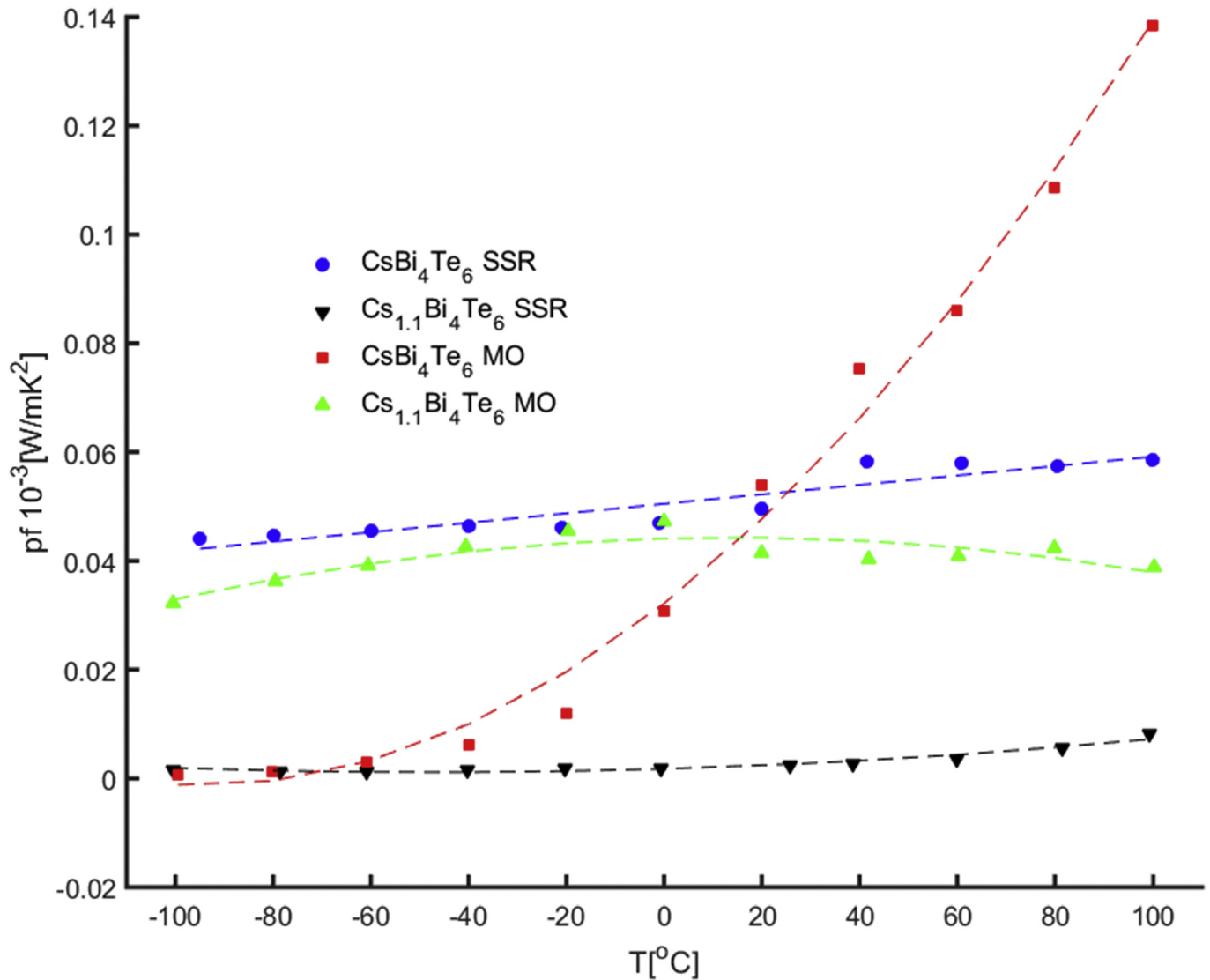


Fig. 5. Temperature dependence of power factor measured for all fabricated samples. Solid lines are guide for eyes only.

Table 2

The summary of microstructural and electrical properties of investigated samples at 32–38 °C.

| Sample | Relative density | Seebeck coefficient, α ($\mu\text{V}/\text{K}$) | Corrected electrical conductivity, σ_{cor} (S/cm) | Thermal conductivity, κ (W/mK) | | | Figure of merit (ZT) |
|--|------------------|---|---|--|------------------------|----------------------|----------------------|
| | | | | Total Corrected κ_{tot} | Electron κ_e | Phonon κ_L | |
| CsBi ₄ Te ₆ -SSR | 0.93 | -40 | 370 | 0.99 | 0.28 | 0.72 | 0.018 |
| Cs _{1.1} Bi ₄ Te ₆ -SSR | 0.89 | -14 | 143 | 0.73 | 0.11 | 0.62 | 0.001 |
| CsBi ₄ Te ₆ -MO | 0.95 | -70 | 154 | 0.43 | 0.10 | 0.33 | 0.054 |
| Cs _{1.1} Bi ₄ Te ₆ -MO | 0.92 | -75 | 71 | 0.93 | 0.06 | 0.87 | 0.013 |

and therefore the ZT. The TE properties of CsBi₄Te₆ are strongly dependent on orientation of grains [1,13]. Polycrystalline sample has a very random grain orientation which results in impairment of the TE properties, thus, a method for controlling the grain orientation is needed.

The highest ZT value equal to 0.054, determined at 32–38 °C was observed in CsBi₄Te₆-MO sample, what may be associated with its composite structure and surprisingly low thermal

conductivity equal to 0.43 W/mK. Unfortunately, ZT values of other samples are quite low.

Nevertheless, the CsBi₄Te₆ phase was successfully obtained. Generally speaking, the investigations have shown that it is possible to fabricate a CsBi₄Te₆ material using methods based on a low temperature reduction of melted or mixed oxides in hydrogen.

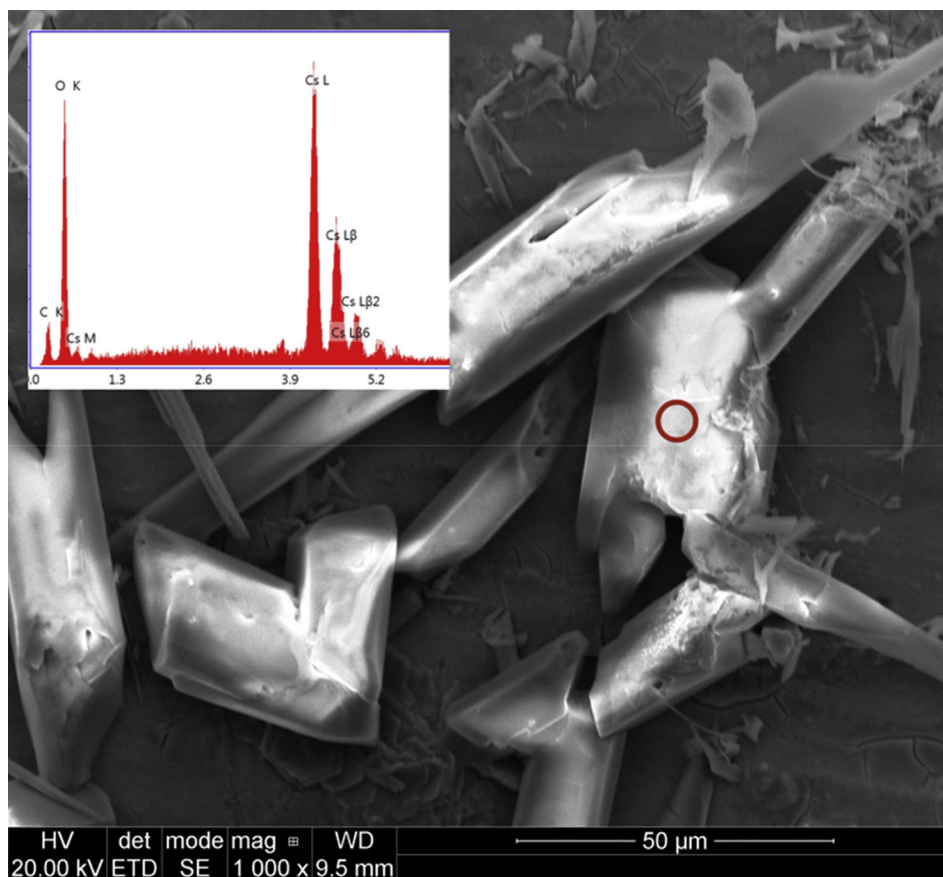


Fig. 6. SEM image of the precipitation on the surface of the sample. Inset: the EDX spectrum of the marked crystal of cesium hydroxide.

Acknowledgments

Authors would like to acknowledge Mr Marcin Stiburski for his help in sample preparation.

This work was supported by the National Science Council under the grant No. NCN 2016/21/B/ST8/03193.

References

- [1] Duck-Young Chung, Tim P. Hogan, Melissa Rocci-Lane, Paul Brazis, John R. Ireland, Carl R. Kannewurf, Marina Bastea, Ctirad Uher, Mercouri G. Kanatzidis, A new thermoelectric material: CsBi_4Te_6 , *J. Am. Chem. Soc.* 126 (20) (2004) 6414–6428, <https://doi.org/10.1021/ja039885f>.
- [2] G.A. Slack, *CRC Handbook of Thermoelectrics*, CRC Press, Boca Raton, 1995, p. 407.
- [3] Y. Pei, J. Lensch-Falk, E.S. Toberer, D.L. Medlin, G.J. Snyder, High thermoelectric performance in PbTe due to large nanoscale Ag_2Te precipitates and La doping, *Adv. Funct. Mater.* 21 (2011) 241–249, <https://doi.org/10.1002/adfm.201000878>.
- [4] S.K. Mishra, S. Satpathy, O. Jepsen, Electronic structure and thermoelectric properties of bismuth telluride and bismuth selenide, *J. Phys. Condens. Matter* 9 (2) (1997) 461.
- [5] O. Yamashita, S. Tomiyoshi, K. Makita, Bismuth telluride compounds with high thermoelectric figures of merit, *J. Appl. Phys.* 93 (1) (2003) 368–374, <https://doi.org/10.1063/1.1525400>.
- [6] T. Schröder, T. Rosenthal, N. Giesbrecht, M. Nentwig, S. Maier, H. Wang, et al., Nanostructures in Te/Sb/Ge/Ag (TAGS) thermoelectric materials induced by phase transitions associated with vacancy ordering, *Inorg. Chem.* 53 (14) (2014) 7722–7729, <https://doi.org/10.1021/ic5010243>.
- [7] G. Joshi, H. Lee, Y. Lan, X. Wang, G. Zhu, D. Wang, et al., Enhanced thermoelectric figure-of-merit in nanostructured p-type silicon germanium bulk alloys, *Nano Lett.* 8 (12) (2008) 4670–4674, <https://doi.org/10.1021/nl8026795>.
- [8] M.S. Toprak, C. Stiewe, D. Platzek, S. Williams, L. Bertini, E. Müller, C. Gatti, Y. Zhang, M. Rowe, M. Muhammed, The impact of nanostructuring on the thermal conductivity of thermoelectric CoSb_3 , *Adv. Funct. Mater.* 14 (2004) 1189–1196, <https://doi.org/10.1002/adfm.200400109>.
- [9] G. Nolas, J.L. Cohn, G.A. Slack, S.B. Schujman, Semiconducting Ge clathrates: promising candidates for thermoelectric applications, *Appl. Phys. Lett.* 73 (2) (1998) 178–180, <https://doi.org/10.1063/1.121747>.
- [10] B. Du, H. Li, J. Xu, X. Tang, C. Uher, Enhanced figure-of-merit in Se-doped p-type AgSbTe_2 thermoelectric compound, *Chem. Mater.* 22 (19) (2010) 5521–5527, <https://doi.org/10.1021/cm101503y>.
- [11] Y. Miyazaki, K. Kudo, M. Akoshima, Y. Ono, Y. Koike, T. Kajitani, Low-temperature thermoelectric properties of the composite crystal $[\text{Ca}_2\text{CoO}_{3.34}]_x[\text{CoO}_2]_{1-x}$, *Jpn. J. Appl. Phys.* 39 (6A) (2000) L531, <https://doi.org/10.1143/JJAP.39.L531>.
- [12] Y.S. Hor, A. Richardella, P. Roushan, Y. Xia, J.G. Checkelsky, A. Yazdani, et al., p-type Bi_2Se_3 for topological insulator and low-temperature thermoelectric applications, *Phys. Rev. B* 79 (19) (2009) 195208, <https://doi.org/10.1103/PhysRevB.79.195208>.
- [13] D.Y. Chung, S.D. Mahanti, W. Chen, C. Uher, M.G. Kanatzidis, Anisotropy in thermoelectric properties of CsBi_4Te_6 , in: *MRS Proceedings*, vol. 793, Cambridge University Press, 2003, <https://doi.org/10.1557/PROC-793-S6.1>, S6–1.
- [14] A. Datta, G.S. Nolas, Solution-based synthesis and low-temperature transport properties of CsBi_4Te_6 , *ACS Appl. Mater. Interfaces* 4 (2) (2012) 772–776, <https://doi.org/10.1021/am201411g>.
- [15] B. Poudel, Q. Hao, Y. Ma, Y. Lan, A. Minnich, B. Yu, et al., High-thermoelectric performance of nanostructured bismuth antimony telluride bulk alloys, *Science* 320 (5876) (2008) 634–638, <https://doi.org/10.1126/science.1156446>.
- [16] J. Yang, T. Aizawa, A. Yamamoto, T. Ohta, Thermoelectric properties of p-type $(\text{Bi}_2\text{Te}_3)_x(\text{Sb}_2\text{Te}_3)_{1-x}$ prepared via bulk mechanical alloying and hot pressing, *J. Alloy. Compd.* 309 (1) (2000) 225–228, [https://doi.org/10.1016/S0925-8388\(00\)01063-X](https://doi.org/10.1016/S0925-8388(00)01063-X).
- [17] H. Wang, J.F. Li, C.W. Nan, M. Zhou, W. Liu, B.P. Zhang, T. Kita, High-performance $\text{Ag}_{0.8}\text{Pb}_{18+x}\text{SbTe}_{20}$ thermoelectric bulk materials fabricated by mechanical alloying and spark plasma sintering, *Appl. Phys. Lett.* 88 (9) (2006) 092104, <https://doi.org/10.1063/1.2181197>.
- [18] C.H. Kuo, C.S. Hwang, M.S. Jeng, W.S. Su, Y.W. Chou, J.R. Ku, Thermoelectric transport properties of bismuth telluride bulk materials fabricated by ball milling and spark plasma sintering, *J. Alloy. Compd.* 496 (1) (2010) 687–690, <https://doi.org/10.1016/j.jallcom.2010.02.171>.
- [19] Y. Kumashiro, K. Nakamura, K. Sato, M. Ohtsuka, Y. Ohishi, M. Nakano, Y. Doi, The properties of Bi-Sb thin films prepared by molecular flow region PVD process, *J. Solid State Chem.* 177 (2) (2004) 533–536, <https://doi.org/10.1016>

- [j.jssc.2003.05.003](https://doi.org/10.1016/j.jssc.2003.05.003).
- [20] Y. Kumashiro, T. Yokoyama, Y. Ando, Thermoelectric properties of boron and boron phosphide CVD wafers, in: Thermoelectrics, 1998. Proceedings ICT 98. XVII International Conference on, IEEE, 1998, May, pp. 591–594. <https://doi.org/10.1109/ICT.1998.740448>.
- [21] H. Lin, H. Chen, J.S. Yu, Y.J. Zheng, P.F. Liu, M.A. Khan, L.M. Wu, CsBi₄Te₆: a new facile synthetic method and mid-temperature thermoelectric performance, Dalton Trans. 45 (30) (2016) 11931–11934, <https://doi.org/10.1039/C6DT02109C>.
- [22] B. Bochentyn, J. Karczewski, T. Miruszewski, B. Kusz, Structure and thermoelectric properties of Bi–Te alloys obtained by novel method of oxide substrates reduction, J. Alloy. Compd. 646 (2015) 1124–1132, <https://doi.org/10.1016/j.jallcom.2015.06.127>.
- [23] B. Bochentyn, T. Miruszewski, J. Karczewski, B. Kusz, Thermoelectric properties of bismuth antimony telluride alloys obtained by reduction of oxide reagents, Mater. Chem. Phys. 177 (2016) 353–359, <https://doi.org/10.1016/j.matchemphys.2016.04.039>.
- [24] B. Kusz, T. Miruszewski, B. Bochentyn, M. Łapiński, J. Karczewski, Structure and thermoelectric properties of Te-Ag-Ge-Sb (TAGS) materials obtained by reduction of melted oxide substrates, J. Electron. Mater. 45 (2) (2016) 1085–1093, <https://doi.org/10.1007/s11664-015-4251-1>.
- [25] B. Bochentyn, J. Karczewski, T. Miruszewski, B. Kusz, Novel method of metal – oxide glass composite fabrication for use in thermoelectric devices, Mater. Res. Bull. 76 (2016) 195–204.
- [26] D.A.G. Bruggeman, Berechnung verschiedener physikalischer Konstanten von heterogenen Substanzen. I. Dielektrizitätskonstanten und Leitfähigkeiten der Mischkörper aus isotropen Substanzen, Ann. Phys. 4016 (1935) 636–664.
- [27] K.W. Schlichting, N.P. Padture, P.G. Klemens, Thermal conductivity of dense and porous yttria-stabilized zirconia, J. Mater. Sci. 36 (12) (2016) 3003–3010.

